

Effect of printing temperature on the viability of *Lactiplantibacillus plantarum* Dad-13 in protein-based 3D food printing product

Pertiwi, A.R.A., Ristiarini, S., Trisnawati, C.Y., Nugerahani, I. and *Srianta, I.

Department of Food Technology, Faculty of Agricultural Technology, Widya Mandala Surabaya Catholic University, Jalan Dinoyo 42-44, Surabaya, Indonesia 60265

Article history:

Received: 8 December 2024

Received in revised form: 18 December 2024

Accepted: 31 May 2025

Available Online: 12 December 2025

Keywords:

Lactiplantibacillus plantarum

Dad-13,

Viability,

Temperature,

3DFP,

Food-ink,

Microstructure

DOI:

[https://doi.org/10.26656/fr.2017.9\(6\).267](https://doi.org/10.26656/fr.2017.9(6).267)

Abstract

Heightened awareness for healthy, nutritious, and sustainable food has emerged post-pandemic. The application of 3D food printing (3DFP) technology holds significant potential for producing functional and sustainable food products. This study aimed to investigate the effect of printing temperatures on the viability of *Lactiplantibacillus plantarum* Dad-13 within protein-based 3D-printed food products. The protein-based food-ink was formulated with defatted tempeh flour, isolated soy protein, probiotic culture *L. plantarum* Dad-13, gelatine and sodium alginate. The 3DFP used in this study was an extrusion-based Foodbot 3D Food Printer, with the following conditions: 2 mm nozzle, 7 mm/s printing speed, and dimensions of 150×150×70 mm. Different printing temperatures were applied (30°C, 35°C, 40°C, 45°C, and 50°C). The printed results were analyzed for probiotic viability and microstructure. *Lactiplantibacillus plantarum* Dad-13 viability in the 3DFP products ranged from 8.8004 to 10.2453 log CFU/g. The printing temperature significantly affected the viability of *L. plantarum* Dad-13 within protein-based 3DFP products. Probiotic viability decreased with increasing printing temperature from 30°C to 50°C. Microscopic observations revealed that elevated temperatures decrease in cell size and the appearance of damaged or incomplete cells. Microstructural analysis revealed variations in matrix compactness within the 3DFP samples, influenced by printing temperature. Higher printing temperatures lead to greater exposure of the probiotic bacteria to direct heat stress. This direct heat exposure contributes to the significant decrease in probiotic viability. Printing temperature of 30°C was the most suitable temperature to produce protein-based 3DFP product.

1. Introduction

The COVID-19 pandemic has significantly altered global food consumption patterns. Heightened awareness of the importance of healthy, nutritious, and sustainable food has emerged post-pandemic. This has spurred innovation within the food industry, notably through the adoption of 3D food printing (3DFP) technology. It offers a novel and efficient approach to food production, enabling the creation of complex and precisely designed foods while facilitating customized product formulations and nutritional profiles to meet individual needs. The application of 3DFP technology holds significant potential for reducing food waste and developing more appealing food products (Wong *et al.*, 2022). Furthermore, 3DFP enables the production of edible packaging materials, such as films and coatings, that come into direct contact with food, thereby minimizing packaging waste (Hakim *et al.*, 2023). Extrusion-based

printing is the most widely employed 3DFP method. In this technique, a food-ink, formulated with specific materials, is loaded into a syringe and extruded through a nozzle. During extrusion, the food-ink is heated to its melting point and subjected to pressure applied by a pump or plunger within the syringe. Key characteristics of a suitable food-ink include the ability to flow smoothly through the nozzle and subsequently solidify after deposition (Sun *et al.*, 2018). Optimal printability and dimensional stability are crucial during printing, post-printing, and subsequent storage. Achieving these characteristics necessitates careful adjustment of the printing temperature.

Previous research has demonstrated the criticality of printing temperature for various food-ink formulations. Chen *et al.* (2022) observed weak interlayer cohesion in protein-based food-ink printed at 25°C, leading to poor printing accuracy. Liu *et al.* (2020) reported a decrease

*Corresponding author.

Email: srianta@ukwms.ac.id

in viscosity and increased dripping in carbohydrate-based mashed potato food-ink printed at 55°C, compromising the extrusion process. In contrast, Huang *et al.* (2023) found that chocolate-based food-ink requires a printing temperature of 60°C, aligned with its melting point. Temperatures below 60°C were shown to negatively impact the flowability and printability of chocolate-based food inks. Therefore, the selection of printing temperature must be carefully considered in relation to the specific food-ink material.

Commonly employed food-ink materials in 3DFP applications include chocolate (Huang *et al.*, 2023), mashed potato (Liu *et al.*, 2020), cereal-based materials such as wheat flour dough (Zhang *et al.*, 2018), and soy protein isolate (Chen *et al.*, 2019), a widely utilized protein source. Compared to chocolate, carbohydrate, and protein-based food inks, the latter often require the addition of hydrocolloids to enhance stability during and after printing. Chen *et al.* (2019) identified gelatin and sodium alginate as effective hydrocolloids for improving food-ink printability. Chen *et al.* (2022) demonstrated the beneficial effects of gelatin and sodium alginate on the gelation properties, water binding capacity, and emulsification ability of soy protein. This study utilizes a soy protein isolate-based food-ink incorporating gelatin and sodium alginate. Soy protein isolate (SPI) can be utilized as a food-ink material due to its protein composition. SPI comprises two dominant globular protein fractions: 7S and 11S globulins. The 7S fraction significantly influences gel elasticity, while the 11S fraction contributes to gel hardness and firmness (Lyu *et al.*, 2022). Preliminary investigations revealed that SPI exhibits a high viscosity, necessitating the incorporation of additional ingredients to enhance its flowability. Defatted tempeh flour (DTF) at 4% (w/v) was included to reduce viscosity and improve the rheological properties of the food-ink. This fat reduction step was implemented to minimize the fat content of tempeh flour (initially 24.7%), which can hinder the dissolution of tempeh flour within the food-ink matrix (Bastian *et al.*, 2013). Probiotic cultures were also incorporated into the food-ink. *Lactiplantibacillus plantarum* Dad-13, isolated from fermented buffalo milk (dadih) in West Sumatra (Rahayu *et al.*, 2016), was selected.

This study employed a food-ink formulation comprising DTF, SPI, *L. plantarum* Dad-13, sodium alginate, and gelatin to achieve optimal printability of a protein-based 3DFP product, which is a semi-finished food and expected to have functional properties. Jannah *et al.* (2022) demonstrated the survival of *L. plantarum* Dad-13 in coffee products stored at 30°C under vacuum packaging, with a viability exceeding 6 log CFU/g after 50 days. Chen *et al.* (2022) reported instability and

collapse of printed objects at 25°C. Previous studies have also highlighted the influence of printing temperature on probiotic viability (Gardiner *et al.*, 2000; Zhang *et al.*, 2018). While previous studies have investigated the viability of *L. plantarum* Dad-13 at 30°C storage temperatures, its viability under the elevated temperatures encountered during direct product contact during 3DFP remains unexplored. Therefore, this study aimed to investigate the impact of varying printing temperatures (30°C, 35°C, 40°C, 45°C, and 50°C) on the viability of *L. plantarum* Dad-13 within 3D-printed food products fabricated using a food-ink matrix comprising defatted tempeh flour and soy protein isolate.

2. Materials and methods

2.1 Materials

The ingredients of 3D food printing food-ink consist of defatted tempeh flour (DTF), Isolated soy protein (ISP), sodium alginate, gelatin (bloom index 200), and probiotic culture *L. plantarum* Dad-13 (10^{14} CFU/g). Isolated soy protein, sodium alginate, and gelatin were purchased from the local market. The probiotic culture *L. plantarum* Dad-13 (10^{14} CFU/g) was purchased from the Food and Nutrition Culture Collection (FNCC), Universitas Gadjah Mada, Indonesia. For preparing DTF, hygienic tempeh purchased from the local market was sliced, steam blanched at 90°C for 2 min, dried at 60°C for 8 h, then crushed and sieved at 70 mesh with a Tyler sieve shaker. The obtained tempeh flour was defatted with hexane at room temperature for 2 h, then dried at 60°C for 8 h.

2.2 Preparation of food-ink and 3D food printing

Food ink was made according to the procedure outlined by Chen *et al.* (2019). The mixture of ISP, DTF, probiotic culture *L. plantarum* Dad-13 (10^{14} CFU/g) with gelatin and sodium alginate was prepared as follows. Firstly, the sodium alginate solution was prepared by dissolving sodium alginate into distilled water (pH around 6.8) with a stirrer for 2 h to make the final concentration of 0.5% (w/v). Secondly, gelatin was added to the sodium alginate solution to reach a concentration of 10% (w/v), and the mixture was incubated in 45°C waterbath for 1 h. Thirdly, ISP and DTF were added into the gelatin and sodium alginate solution to reach a concentration of 20% (w/v) and 4% (w/v) and the paste was mixed manually in a waterbath at about 100 rpm for 5 min. All the prepared mixtures were stored at 4°C overnight and heated to 45°C. After being heated, and the paste is in a liquid state, probiotic culture *L. plantarum* Dad-13 0.1% (w/v) can be added. The 3DFP used in this study is an extrusion-based Foodbot 3D Food Printer, with the following conditions:

2 mm nozzle, 7 mm/s printing speed, and dimensions of 150x150x70 mm. Different printing temperatures were applied 30°C (P1), 35°C (P2), 40°C (P3), 45°C (P4), and 50°C (P5). The printed results were analyzed for probiotic viability and microstructure.

2.3 *Lactiplantibacillus plantarum* Dad-13 viability analysis

The probiotic viability of food-ink and printed object were analyzed according to Jannah *et al.* (2022). The sample (1 g) was crushed using a sterile mortar and pestle. The crushed sample was transferred to a test tube containing 9 mL of 0.85% NaCl diluent solution, resulting in a 10^{-1} dilution. Serial dilutions of ten-fold were subsequently performed, with 1 mL of each dilution transferred to the next test tube and vortexed until a 10^{-12} dilution was achieved. Immediately following dilutions from 10^{-6} to 10^{-12} , 1 mL aliquots were aseptically transferred from each dilution tube to duplicate sterile Petri dishes. MRS Agar medium, pre-warmed to 50°C, was then poured into the Petri dishes. The plates were gently mixed by rotating them in a figure-eight pattern and allowed to solidify. Incubation was carried out at 37°C for 48 h. Colony counts were determined using a colony counter. The *L. plantarum* Dad-13 bacterial colonies exhibited a characteristic round morphology, white color, and smooth edges (Putrayana *et al.*, 2023).

2.4 Microscopic characteristics of *Lactiplantibacillus plantarum* Dad-13 observation

Gram staining of *L. plantarum* Dad-13 was performed according to Kurnia *et al.* (2020). A loopful (1-2) of sterile distilled water was aseptically transferred to the clean slide, followed by the addition of a loopful of *L. plantarum* Dad-13. This mixture was then heat-fixed. Crystal violet solution (2-3 drops) was applied to the slide and allowed to stain for 2 min. The slide was then rinsed with running water and air-dried. Subsequently, Gram's iodine solution (2-3 drops) was applied and left for 1 min, followed by rinsing with water and air-drying. Decolorization was achieved by applying 2-3 drops of a 7:3 ethanol-acetone mixture and rinsing with water until the purple color ceased to run. Finally, safranin solution (0.5%, 2-3 drops) was applied as a counterstain for 30 seconds, followed by rinsing with water and air-drying. The stained slide was then observed under a microscope. Lactic acid bacteria were identified by their characteristic purple, rod-shaped morphology.

2.5 Microstructure analysis

Microstructural analysis was conducted using a Scanning Electron Microscope (SEM). The 3DFP

sample was initially ground. Subsequently, it was subjected to Critical Point Drying to remove residual moisture. Prior to SEM observation, the sample was coated with a thin layer of Au-Pd (gold-palladium). This coating enhances sample conductivity, facilitating electron flow and resulting in clearer and more accurate images (Setyaningsih *et al.*, 2017). The thin coating layer minimizes obscuration of surface details, enabling high-resolution imaging. SEM operates by focusing a beam of electrons onto the sample surface. The interaction between the electron beam and the sample generates various signals, including secondary electrons, which are detected to form an image. The magnification can be adjusted by manipulating the electron beam and focusing lenses. For this study, the 3DFP sample was observed under SEM at magnifications of 1000x and 2000x. Particle diameter measurements were subsequently analyzed using ImageJ software.

2.6 Statistical analysis

The data were expressed as mean \pm standard deviations (SD) from five individual repetitions. The obtained data were statistically analyzed with analysis of variance (ANOVA) at $\alpha = 0.05$ and Duncan's multiple range tests (DMRT) at $\alpha = 0.05$ using SPSS software (IBM, version 25, USA).

3. Results and discussion

3.1 *Lactiplantibacillus plantarum* Dad-13 viability

Lactiplantibacillus plantarum Dad-13 viability in the 3DFP products ranged from 8.8004 to 10.2453 log CFU/g. The viability at different printing temperatures can be seen in Figure 1. The printing temperature significantly affected the viability of *L. plantarum* Dad-13 within protein-based 3DFP products.

As depicted in Figure 1, a decline in bacterial viability was observed with increasing printing temperature. At 30-35°C, probiotic viability remained high, reaching 10^{10} CFU/g. This aligns with the findings of Wardani *et al.* (2017), who reported that *L. plantarum* Dad-13 exhibits optimal growth within the temperature range of 30-37°C, classifying it as a mesophilic bacterium. A significant decrease in probiotic viability was observed between 35°C and 40°C, likely attributed to temperatures exceeding the optimal growth range. Wardani *et al.* (2017) also reported a gradual decline in *L. plantarum* Dad-13 viability at temperatures above 40°C. Consequently, at printing temperatures of 40°C and above, a continued reduction in viability to 10^9 CFU/g was observed. At 50°C, probiotic viability plummeted to 2 log CFU/g, primarily due to direct contact between the probiotic-laden food-ink and elevated temperatures. Several studies have reported that the optimal growth

temperature for various probiotic strains, including *Bifidobacteria* and *Lactobacillus* species, typically falls within the range of 37-43°C (Boylston et al., 2004; Lee and Salminen, 2009; Korbekandi et al., 2011). High-temperature processing, particularly in the range of 45-50°C, can significantly impact probiotic survival (Tripathi and Giri, 2014). In response to initial heat exposure, probiotics activate stress response mechanisms, including the synthesis of small heat-shock proteins (sHSPs), which are ATP-independent chaperone molecules (Petrof et al., 2004; Rocchetti et al., 2023). sHSPs play a crucial role in protecting cellular structures by refolding denatured proteins and maintaining membrane integrity (Angelis et al., 2004). However, at elevated temperatures (40-50°C), the protective capacity of sHSPs may become insufficient. This temperature increase coincided with a decline in viability, further supported by microscopic observations of cellular damage to probiotic bacteria.

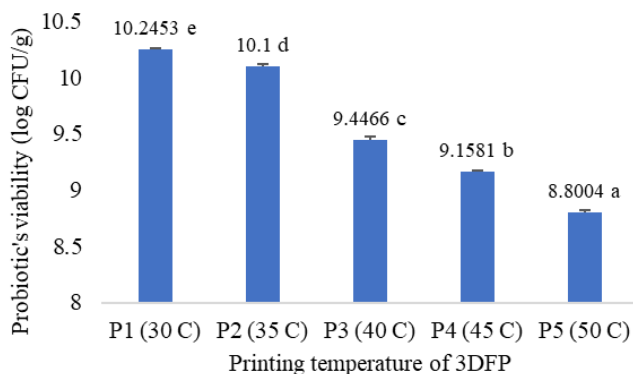


Figure 1. The probiotic *Lactiplantibacillus plantarum* Dad-13 viability at different temperatures in protein-based 3DFP product (n = 5). Values with different superscripts are statistically significantly different (DMRT at $\alpha = 0.05$).

Elevated printing temperatures and prolonged printing times (12 min per treatment) resulted in bacterial cell injury. Sublethally injured cells may exhibit damage to cell membranes, cell walls, DNA, RNA, ribosomes, and essential enzymes (Kurniati et al., 2020; Maehata et al., 2021). Heat stress can disrupt the lipid bilayer, leading to increased membrane permeability. This disruption can result in the leakage of intracellular components, such as ions and metabolites, and impair enzymatic reactions (Hastuti et al., 2016). During heat exposure, protein denaturation occurs, altering the three-dimensional structure of proteins and compromising their functionality. This consequently leads to a significant reduction in metabolic activity. Decreased metabolic activity diminishes ATP production, ultimately hindering cell growth and reproduction, culminating in cell lysis and bacterial cell death. Studies have demonstrated that high temperatures can rapidly inactivate probiotic strains. For instance, *Lactobacillus reuteri* C-10 has been shown to exhibit complete destruction within 15 minutes

at 70°C (Azim et al., 2012). Therefore, increasing printing temperature significantly reduces the viability of probiotic bacterial cells.

3.2 Microscopic characteristics of *Lactiplantibacillus plantarum* Dad-13

Microscopic characterization was conducted using Gram staining to assess the impact of printing temperature on cell morphology. Gram staining revealed rod-shaped, purple-colored cells, consistent with previous findings by Putrayana et al. (2023). They observed that *L. plantarum* Dad-13 grown on MRS Agar exhibited round, white colonies, while microscopic examination revealed rod-shaped, purple-colored cells. The purple coloration following crystal violet staining indicates Gram-positive bacteria. This observation aligns with the findings of Bergey and Holt (2000), who reported that Gram-positive bacteria possess thick peptidoglycan cell walls, facilitating the retention of crystal violet stain. Microscopic observations using Gram staining were also performed to identify potential cellular damage in probiotic bacteria. Figure 2 summarizes the microscopic observations of *L. plantarum* Dad-13 at various printing temperatures under 1000× magnification.

Microscopic observations revealed that at 30-35°C, probiotic cells exhibited a typical rod-shaped morphology. As reported by Hastuti et al. (2016), elevated temperatures can induce denaturation of bacterial cell wall proteins. Consistent with these findings, at 40-45°C, a decrease in cell size and the appearance of damaged or incomplete cells were observed. Darmastuti et al. (2021) identified FtsL, a protein supported by the murein hydrolase enzyme, as a key component in maintaining the cell wall structure of *L. plantarum* Dad-13. In response to thermal stress, FtsL interacts with murein hydrolase to facilitate cellular adaptation. Additionally, D-alanine transport regulator (DltR) and D-alanine ligase (DltS) play crucial roles in maintaining cell shape (Darmastuti et al., 2021). At 50°C, significant cell wall structural protein denaturation was evident. This denaturation disrupts the interaction between the cell membrane and the cytoskeleton, leading to cell rounding. This morphological alteration is likely attributed to cytoskeletal damage, which plays a critical role in maintaining cell shape. Furthermore, the instability of the D-alanylation system components, DltR and DltS, which are involved in modifying the bacterial cell wall by incorporating D-alanine into teichoic acid, may contribute to this morphological distortion. The instability of this system is likely a consequence of thermal stress exceeding the optimal growth temperature of the probiotic. At 50°C, cell rounding becomes prominent. Prolonged exposure to elevated temperatures

can compromise cell membrane integrity, leading to increased permeability and the leakage of intracellular components, such as nutrients and enzymes, ultimately resulting in cell death (Hastuti *et al.*, 2016). This membrane disruption can be attributed to the loss of membrane fluidity and increased permeability, potentially due to the denaturation of membrane proteins.

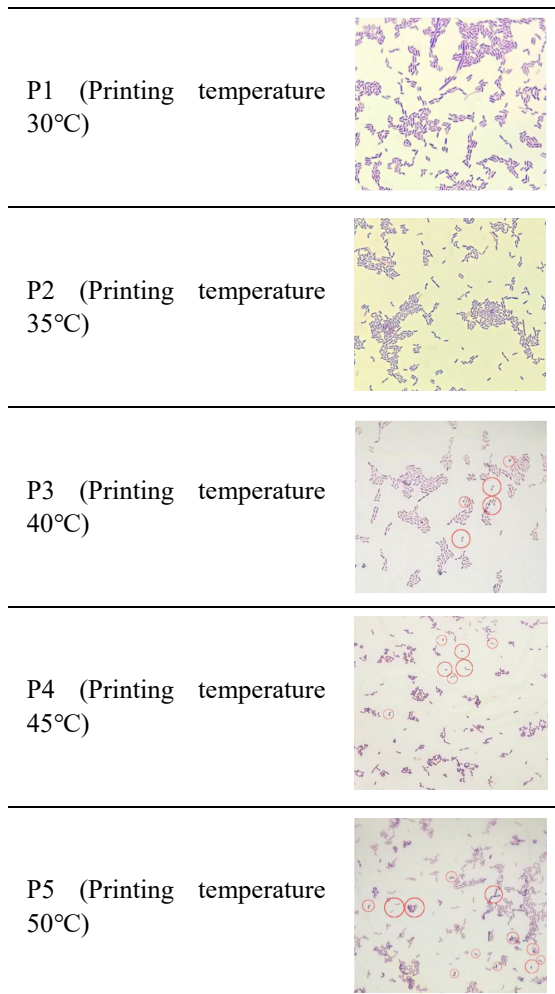


Figure 2. Microscopic observations of *Lactiplantibacillus plantarum* Dad-13 at various printing temperatures under 1000 \times magnification.

3.3 Microstructure of 3D food printing products

Microstructural analysis was performed on 3DFP products that had been printed at various printing temperatures using a Scanning Electron Microscope (SEM). The results of the microstructural analysis of soy-based probiotic 3DFP products can be seen in Figure 3.

Microstructural analysis revealed variations in matrix compactness within the 3DFP samples, influenced by printing temperature. The 3DFP sample printed at 30 $^{\circ}$ C exhibited a rougher cross-section compared to those printed at 40 $^{\circ}$ C and 50 $^{\circ}$ C. This observation can be attributed to weaker interactions between protein particles at 30 $^{\circ}$ C, primarily relying on hydrogen bonds, leading to a more dispersed protein distribution. Additionally, the presence of large pores

within the 3DFP sample printed at 30 $^{\circ}$ C may be associated with the higher mechanical strength and viscosity of the food-ink at this temperature. At 30 $^{\circ}$ C, gelatin likely exists in a semi-solid or gel state (Mad-Ali *et al.*, 2017), limiting its flowability and interaction with other components. Although sodium alginate, SPI, and tempeh require sufficient hydration to form a gel-like structure, the low temperature may hinder optimal hydration and interaction. However, at 30 $^{\circ}$ C, the incorporated *L. plantarum* Dad-13 probiotics may experience enhanced protection from heat stress, as the hydrogel and other components act as a thermal barrier. In the micrograph of the 3DFP sample printed at 40 $^{\circ}$ C, tighter intermolecular bonds were observed between protein particles, with a distinct gelatin layer surrounding the interconnected protein network. At this temperature, gelatin transitions to a liquid state, enhancing its binding properties and facilitating the formation of a more cohesive matrix. Chen *et al.* (2022) reported that gelatin forms a stable 3D network within the temperature range of 35-45 $^{\circ}$ C, effectively trapping protein particles and resulting in a relatively stable 3D structure upon cooling to room temperature (approximately 25 $^{\circ}$ C). However, the increased fluidity at 40 $^{\circ}$ C may have allowed for greater movement of the hydrogel and other components within the matrix prior to solidification, potentially exposing the probiotics to more direct heat stress, contributing to the observed decrease in probiotic viability compared to the 30 $^{\circ}$ C sample. The micrograph

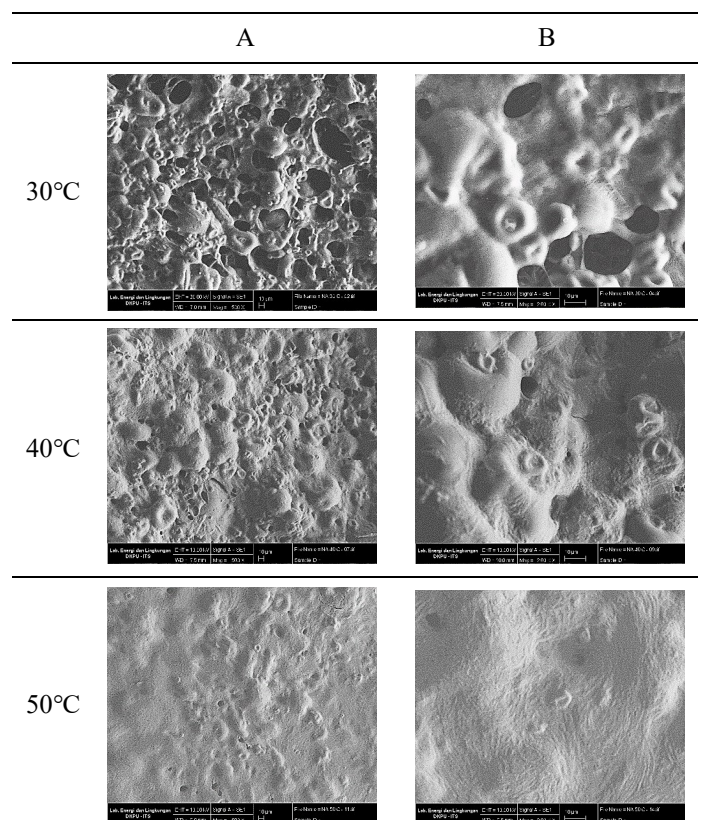


Figure 3. Microstructure observation with Scanning Electron Microscope at temperatures 30 $^{\circ}$ C, 40 $^{\circ}$ C, and 50 $^{\circ}$ C. (A) 1000 \times magnification and (B) 2000 \times magnification.

of the 3DFP sample printed at 50°C demonstrated even tighter bonds between protein particles, likely due to the complete liquefaction of gelatin at this temperature. The liquid state of gelatin at 50°C facilitates improved interaction and integration with other components, resulting in a more uniform microstructure. Moreover, the elevated temperature likely enhanced the hydration of sodium alginate and SPI, promoting swelling and contributing to a more interconnected matrix (Zhang et al., 2024). The addition of gelatin and sodium alginate to the food-ink significantly improved its flowability, enabling smooth extrusion through the nozzle. Food-ink viscosity is inversely related to printing temperature. Higher printing temperatures reduce viscosity, facilitating easier extrusion. However, this increased fluidity at higher temperatures can also lead to greater exposure of the probiotic bacteria to direct heat stress, as the hydrogel and other components exhibit increased mobility within the matrix, providing less thermal protection. This direct heat exposure contributes to the significant decrease in probiotic viability, reaching up to 2 log CFU/g at 50°C.

4. Conclusion

The printing temperature significantly affected the viability of *L. plantarum* Dad-13 within protein-based 3DFP products. Probiotic viability decreased with increasing printing temperature from 30°C to 50°C. At 30-35°C, probiotic viability remained high, reaching 10 log CFU/g. At printing temperatures of 40°C and above, a continued reduction in viability to 10⁹ CFU/g was observed. At 50°C, probiotic viability plummeted to 2 log CFU/g. Microscopic observations and microstructural analysis supported the results of probiotic viability analysis. Lower printing temperatures resulted in a rougher cross-section structure of protein-based 3DFP products, which may be associated with lower mobility of hydrogel and other components, thus providing more thermal protection to the probiotic. Future studies should include rheological analysis to confirm this. Optimum baking temperature and sensory analysis on the baked product are also needed for further development of this product.

Conflict of interest

The authors declare no conflict of interest.

Acknowledgements

Thanks to Direktorat Riset dan Pengabdian Masyarakat Deputy Bidang Penguatan Riset dan Pengembangan Kementerian Riset dan Teknologi/ Badan Riset dan Inovasi Nasional for financial support to this

research work with contract number: 109/E5/PG.02.00.PL/2024. Thanks to Arya Wira Dharma for the technical assistance provided during this research work and for writing this article.

References

- Angelis, M.D., Cagno, R.D., Huet, C., Crecchio, C., Fox, P.F. and Gobbetti, M. (2004). Heat Shock Response in *Lactobacillus plantarum*. *Applied And Environmental Microbiology*, 70(3), 1336–1346. <https://doi.org/10.1128/AEM.70.3.1336>
- Azim, H., Kalavathy, R., Julianto, T., Sieo Chin, C. and Ho Wan, Y. (2012). Effect of heat, pH and coating process with stearic acid using a fluidized bed granulator on viability of probiotic *Lactobacillus reuteri* C 10. *African Journal of Biotechnology*, 11 (26), 6857–6865. <https://doi.org/10.5897/ajb11.2984>
- Bastian, F., Ishak, E., Tawali, A. and Bilang, M. (2013). Daya Terima dan Kandungan Zat Gizi Formula Tepung Tempe dengan Penambahan Semi Refined Carrageenan (SRC) dan Bubuk Kakao. *Jurnal Aplikasi Teknologi Pangan*, 2(1), 5–8. Retrieved from [In Bahasa Indonesia].
- Bergey, D.H. and Holt, J.G. (2000). *Bergey's Manual of Determinative Bacteriology*. Philadelphia, USA: Lippincott Williams and Wilkins.
- Boylston, T.D., Vinderola, C.G., Ghoddusi, H.B. and Reinheimer, J.A. (2004). Incorporation of *bifidobacteria* into cheeses: challenges and rewards. *International Dairy Journal*, 14(5), 375-387. <https://doi.org/10.1016/j.idairyj.2003.08.008>
- Chen, J., Mu, T., Goffin, D., Blecker, C., Richard, G., Richel, A. and Haubruge, E. (2019). Application of soy protein isolate and hydrocolloids based mixtures as promising food material in 3D food printing. *Journal of Food Engineering*, 261(3), 76–86. <https://doi.org/10.1016/j.jfoodeng.2019.03.016>
- Chen, J., Sun, H., Mu, T., Blecker, C., Richel, A., Richard, G., Jacquet, N., Haubruge, E. and Goffin, D. (2022). Effect of temperature on rheological, structural, and textural properties of soy protein isolate pastes for 3D food printing. *Journal of Food Engineering*, 323, 110917. <https://doi.org/10.1016/j.jfoodeng.2021.110917>
- Darmastuti, A., Hasan, P.N., Wikandari, R., Utami, T., Rahayu, E.S. and Suroto, D.A. (2021). Adhesion properties of *Lactobacillus plantarum* dad-13 and *Lactobacillus plantarum* mut-7 on sprague dawley rat intestine. *Microorganisms*, 9(11), 2336. <https://doi.org/10.3390/microorganisms9112336>
- Gardiner, G.E., O'Sullivan, E., Kelly, J., Auty, M.A., Fitzgerald, G.F., Collins, J.K., Ross, R.P. and

- Stanton, C. (2000). Comparative survival rates of human-derived probiotic *Lactobacillus paracasei* and *L. salivarius* strains during heat treatment and spray drying. *Applied and Environmental Microbiology*, 66(6), 2605–2612. <https://doi.org/10.1128/AEM.66.6.2605-2612.2000>
- Hakim, L., Kumar, L. and Gaikwad, K. (2023). Screen printing of catechu (*Senegalia catechu*)/guar gum based edible ink for food printing and packaging applications. *Progress in Organic Coatings*, 182, 107629. <https://doi.org/10.1016/j.porgcoat.2023.107629>
- Hastuti, U.S., Rahmawati, I. and Asna, P.M. (2016). Kajian Daya Antibakteri Beberapa Spesies Kapang Endofit yang Diisolasi dari Tanaman Ginseng Jawa (*Talinum paniculatum* (Jag.) Gaertn). *Proceeding Biology Education Conference*, 13(1), 844–848. [In Bahasa Indonesia].
- Huang, J.H.R., Lim, G.G.C.W., Su, C.H.J. and Ciou, J.Y. (2023). Improvement of 3D white chocolate printing molding effect with oleogels. *Heliyon*, 9(9), e19165. <https://doi.org/10.1016/j.heliyon.2023.e19165>
- Jannah, S.R., Rahayu, E.S., Yanti, R., Suroto, D.A. and Wikandari, R. (2022). Study of Viability, Storage Stability, and Shelf Life of Probiotic Instant Coffee *Lactiplantibacillus plantarum* Subsp. *plantarum* Dad-13 in Vacuum and Nonvacuum Packaging at Different Storage Temperatures. *International Journal of Food Science*, 2022, 1663772. <https://doi.org/10.1155/2022/1663772>
- Korbekandi, H., Mortazavian, A. and Irvani, S. (2011). Technology and stability of probiotic in fermented milks. In *Probiotic and prebiotic foods: Technology, stability and benefits to the human health*, p. 131-169. New York, USA: Nova Science Publishers, Inc.
- Kurnia, M., Amir, H. and Handayani, D. (2020). Isolasi Dan Identifikasi Bakteri Asam Laktat Dari Makanan Tradisional Suku Rejang Di Provinsi Bengkulu: “Lemea.” *Alotrop*, 4(1), 25–32. <https://doi.org/10.33369/atp.v4i1.13705>
- Kurniati, E., Huy, V.T., Anugroho, F., Sulianto, A.A., Amalia, N. and Nadhifa, A.R. (2020). The effect of pH and temperature on disinfection process using microbubble and pressurized carbon dioxide. *Jurnal Pengelolaan Sumberdaya Alam Dan Lingkungan*, 10 (2), 247–256. <https://doi.org/10.29244/jpsl.10.2.247-256>
- Lee, Y.K. and Salminen, S. (2009). *Handbook of probiotics and prebiotics*. New Jersey, USA: John Wiley and Sons.
- Liu, Z., Bhandari, B. and Zhang, M. (2020). Incorporation of probiotics (*Bifidobacterium animalis* subsp. *Lactis*) into 3D printed mashed potatoes: Effects of variables on the viability. *Food Research International*, 128, 108795. <https://doi.org/https://doi.org/10.1016/j.foodres.2019.108795>
- Lyu, B., Li, J., Meng, X., Fu, H., Wang, W., Ji, L., Wang, Y., Guo, Z. and Yu, H. (2022). The Protein Composition Changed the Quality Characteristics of Plant-Based Meat Analogues Produced by a Single-Screw Extruder: Four Main Soybean Varieties in China as Representatives. *Foods*, 11(8), 1112. <https://doi.org/10.3390/foods11081112>
- Mad-Ali, S., Benjakul, S., Prodpran, T. and Maqsood, S. (2017). Characteristics and gelling properties of gelatin from goat skin as affected by drying methods. *Journal of Food Science and Technology*, 54(6), 1646–1654. <https://doi.org/10.1007/s13197-017-2597-5>
- Maehata, H., Arai, S., Iwabuchi, N. and Abe, F. (2021). Immuno-modulation by heat-killed *Lactocaseibacillus paracasei* MCC1849 and its application to food products. *International Journal of Immunopathology and Pharmacology*, 2021, 35. <https://doi.org/10.1177/20587384211008291>
- Petrof, E.O., Kojima, K., Ropeleski, M.J., Musch, M.W., Tao, Y., De Simone, C. and Chang, E.B. (2004). Probiotics inhibit nuclear factor- κ B and induce heat shock proteins in colonic epithelial cells through proteasome inhibition. *Gastroenterology*, 127(5), 1474–1487. <https://doi.org/10.1053/j.gastro.2004.09.001>
- Putrayana, K.D.A.M., Permatasari, A.A.A.P., Lestari, N.K.D. and Sari, N.K.Y. (2023). Karakterisasi Dan Uji Antagonis *Lactobacillus plantarum* Dad-13 Sebagai probiotik Terhadap *Escherichia coli* Dan *Staphylococcus aureus*. *Jurnal Biologi Indonesia*, 19 (1), 93–97. <https://doi.org/10.47349/jbi/19012023/93> [In Bahasa Indonesia].
- Rahayu, E.S., Yogeswara, A., Mariyatun, Windiarti, L., Utami, T. and Watanabe, K. (2016). Molecular characteristics of indigenous probiotic strains from Indonesia. *International Journal of Probiotics and Prebiotics*, 11(2), 109–116.
- Rocchetti, M.T., Bellanger, T., Trecca, M.I., Weidmann, S., Scrima, R., Spano, G., Russo, P., Capozzi, V. and Fiocco, D. (2023). Molecular chaperone function of three small heat-shock proteins from a model probiotic species. *Cell Stress and Chaperones*, 28(1), 79–89. <https://doi.org/10.1007/s12192-022-01309-6>
- Setyaningsih, N.E., Muttaqin, R. and Mar’ah, I. (2017). Optimalisasi Waktu Coating pada Bahan Komposit Alam untuk Karakterisasi Morfologi dengan Scanning Electron Microscopy (SEM) – Energy

- Dispersive X-Ray Spectroscopy (EDX). *Physics Communication*, 1(2), 36–40. <https://doi.org/10.15294/physcomm.v1i2.10777>
- Sun, J., Zhou, W., Yan, L., Huang, D. and Lin, L. (2018). Extrusion-based food printing for digitalized food design and nutrition control. *Journal of Food Engineering*, 220, 1–11. <https://doi.org/https://doi.org/10.1016/j.jfoodeng.2017.02.028>
- Tripathi, M.K. and Giri, S.K. (2014). Probiotic Functional Foods: Survival of Probiotics during Processing and Storage. *Journal of Functional Foods*, 9, 225-241. <https://doi.org/10.1016/j.jff.2014.04.030>
- Wardani, S.K., Cahyanto, M.N., Rahayu, E.S. and Utami, T. (2017). The effect of inoculum size and incubation temperature on cell growth, acid production and curd formation during milk fermentation by *Lactobacillus plantarum* Dad 13. *International Food Research Journal*, 24(3), 921–926.
- Wong, H.C.G., Pant, A., Zhang, Y., Kai Chua, C., Hashimoto, M., Huei Leo, C. and Tan, U.X. (2022). 3D food printing– sustainability through food waste upcycling. *Materials Today: Proceedings*, 70, 627–630. <https://doi.org/https://doi.org/10.1016/j.matpr.2022.08.565>
- Zhang, L., Lou, Y. and Schutyser, M.A.I. (2018). 3D printing of cereal-based food structures containing probiotics. *Food Structure*, 18, 14–22. <https://doi.org/10.1016/j.foostr.2018.10.002>
- Zhang, Z., Huang, M., Shen, K., He, Y. and Liu, Y. (2024). Sodium Alginate–Soy Protein Isolate–Chitosan–Capsaicin–Nanosilver Multifunctional Antibacterial Composite Gel. *Processes*, 12(4), 662. <https://doi.org/10.3390/pr12040662>